CrossMark

Thermal conductivity of low temperature grown vertical carbon nanotube bundles measured using the three-ω method

Sten Vollebregt,[a] Sourish Banerjee, Kees Beenakker, and Ryoichi Ishihara
Delft University of Technology, Delft Institute of Microsystems and Nanoelectronics, Feldmannweg 17, 2628CT Delft, The Netherlands

(Received 10 April 2013; accepted 1 May 2013; published online 15 May 2013)

The thermal conductivity of as-grown vertical multi-walled carbon nanotubes (CNT) bundles fabricated at low temperature (500 °C) was measured using a vertical 3ω-method. For this, CNT were selectively grown inside an oxide opening and sandwiched between two metal electrodes. The validity of the method was confirmed by both measurements as simulations. The measured thermal conductivity of 1.7-3.5 W/mK is significantly lower than values reported before, which is caused by the low quality of the tubes. This clearly indicates that tube quality will be essential when integrating CNT. © *2013 AIP Publishing LLC*. [http://dx.doi.org/10.1063/1.4805069]

Thermal management is a serious issue in modern electronics, hampering their performance and reducing reliability. Vertically aligned carbon nanotubes (CNT) have been suggested as future thermal management material for integrated circuits, both internally in the chip as vertical interconnects (vias),[1,2] as externally as heatsink[3] or thermal interface material (TIM).[4–6] To allow low-cost integration and optimum thermal contact, it is necessary to grow the CNT directly on the desired location.[7] As the allowed thermal budget for back-end integration is limited, the CNT should be grown at low temperatures ($\leq$ 500 °C).

Most data published on the thermal conductivity of CNT are for individual single-walled or multi-walled tubes,[8–13] with reported values as high as 3000 W/mK for both. For bundles of CNT on the other hand, which are required to obtain a low enough electrical and heat resistance,[2] less data are available.[14–18] Moreover, the values for the thermal conductivity reported in the literature vary significantly, ranging from 50 to 5800 W/mK, and are generally one order of magnitude lower than those obtained from individual tubes.

Still, while the data on the thermal conductivity for CNT bundles are available, none of the published results represent CNT directly grown at low temperatures, and at the desired location. Most results are obtained from tubes fabricated using arc-discharge, laser ablation, or high temperature (>700 °C) chemical vapour deposition (CVD). However, none of these production methods are suitable for the actual fabrication of CNT vias or TIM due to the need of full wafer fabrication and low growth temperatures. In order to investigate the impact of fabrication methods on the CNT thermal properties, and to determine if CNT can actually outperform current metals (e.g. Cu), thermal data on low temperature grown CNT are required.

In this work, we measured the thermal conductivity of vertical CNT bundles manufactured between two metal electrodes. The bundle is grown at low temperature (500 °C), and at the desired location using selective growth, requiring no additional process steps after growth except for the top electrode deposition. For the thermal measurements, a vertical 3ω-method was employed, the validity of which was verified using finite elements simulations. We found that the thermal conductivity of low-temperature grown CNT is significantly lower than the values obtained for high quality CNT.

The CNT via test structures are fabricated as specified elsewhere.[19] Shortly, 10 cm Si wafers are covered using sputtering by 500 nm Ti, 50 nm TiN, and another 100 nm Ti (which acts as a sacrificial layer). After this, 3 μm of SiO_2 is deposited using plasma enhanced chemical vapour deposition, and contact openings are etched using dry etching. Then, the sacrificial layer is removed using 1 min 0.55% HF wet etching, and the 5 nm Fe catalyst for CNT growth is evaporated and patterned by lift-off. CNT are then grown using low-pressure CVD (LPCVD) at a temperature of 500 °C, a pressure of 8 kPa, and using gas flows of 700/50 sccm of H_2/C_2H_2. Next, 100 nm of Ti and 3 μm of Al(1% Si) are sputtered over the CNT bundles and patterned with wet etching. Finally, an etch-back to the first metal layer is performed with dry etching, in order to allow direct electrical contact to the bottom electrode. Fig. 1 displays an overview of the fabrication process.

A typical cross-section of an as-fabricated via test structure made by focused ion-beam (FIB) and a scanning electron microscope (SEM) is shown in Fig. 2. CNT density is estimated to be $\sim 10^{11}$ tubes/cm^2, while the diameter is between 10 and 20 nm, with an average of 14 nm.[20] The CNT bundle is well-aligned, with a height of 2.6 μm, which is slightly shorter than the oxide thickness. There is a 100–200 nm gap between the CNT bundle. As the pressure during final metallization, which encapsulates the structures, is in the range of a 1 Pa, we can assume these gaps to be vacuum, effectively isolating the tubes from their surroundings.

Thermal characterisation was performed using an adjusted 3ω-method. Instead of a horizontal bundle suspended over a vacuum gap,[21] a vertical bundle between two electrodes in a (presumable vacuum) opening was measured. This allows direct measurement of the as-grown vertical bundles. In the 3ω-method, a suspended bundle of CNT is excited by a sine current with frequency ω, which induces

[a]Electronic mail: s.vollebregt@tudelft.nl

 © 2013 AIP Publishing LLC

Downloaded 04 Jul 2013 to 131.180.130.178. This article is copyrighted as indicated in the abstract. Reuse of AIP content is subject to the terms at: http://apl.aip.org/about/rights_and_permissions

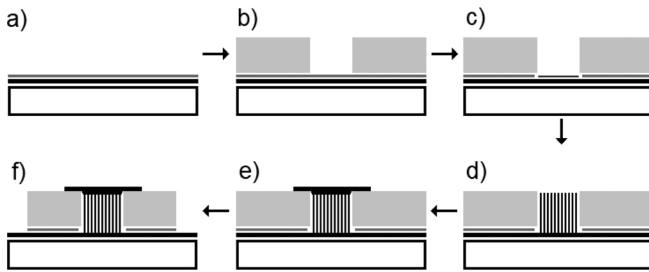

FIG. 1. Overview of fabrication process: step (a) creation of a metal stack on Si wafer consisting of 500 nm Ti, 50 nm TiN, and 100 nm Ti sacrificial layer; (b) deposition of SiO_2 and plasma etching of opening windows; (c) wet sacrificial-layer removal and Fe evaporation; (d) CNT growth at 500 °C using LPCVD; (e) top metal (100 nm Ti, 3 μm Al) sputtering and patterning; (f) etch-back to previous layer.

Joule heating in the specimen with a frequency of 2ω. The 2ω temperature change induces a change in the sample resistance, which interacts with the sine current and creates a third harmonic potential ($V_{3\omega}$) change depending (in the low frequency limit) on the sample properties by[21]

$$V_{3\omega} = \frac{4I^3RR'L}{\pi^4\kappa S} \quad (1)$$

in which I is the rms current, R is the sample resistance, R' is the sample temperature coefficient of resistance (TCR), L is the length of the sample, κ is the thermal conductivity, and S is the cross-sectional area of the sample.

For the electrical characterisation of the wafers, a semi-automatic probe station with a temperature controlled chuck and semiconductor parameter analyser were utilized. The same probe station, in combination with a SR830 lock-in amplifier at high dynamic reserve, was used for the thermal characterisation. As current source, we used the reference output of the lock-in amplifier which was converted by a transconductance amplifier similar to the one used by Choi *et al.*[22]

In order to calculate the thermal conductivity of the CNT bundles, first their electrical properties have to be measured. Full-wafer 4-point probe resistance measurements have been performed, as shown before.[23] To determine the TCR, the wafers with CNT bundles were measured on substrate temperatures ranging from 190 °C to −35 °C. Figure 3 displays the obtained resistances versus substrate temperature, with the resulting TCR calculated using least square fitting of the data.

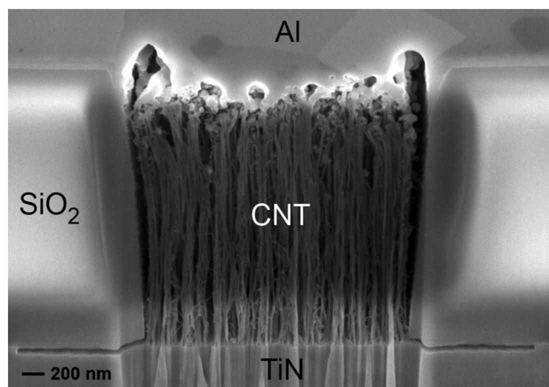

FIG. 2. SEM image of a dual-beam FIB prepared cross-section of a 2 μm wide and 3 μm deep CNT via, CNT length is estimated to be 2.6 μm.

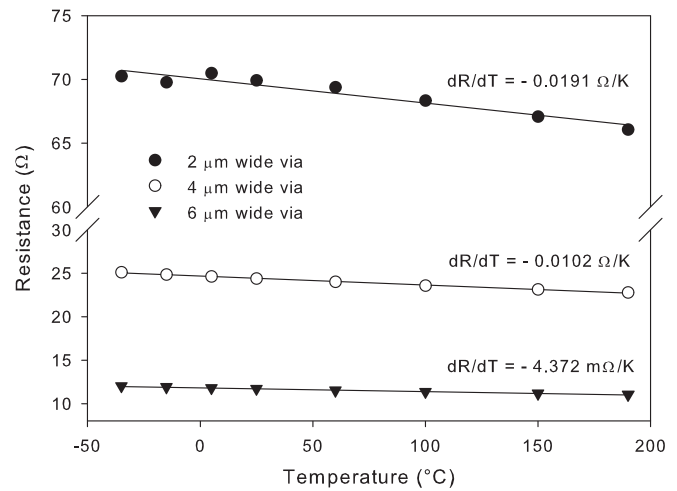

FIG. 3. TCR of 2.6 μm long CNT vias with different widths, determined using least square fitting.

As can be seen, the TCR of the CNT bundles is negative. For CNT, there are two competing thermal dependent mechanisms that influence the CNT resistance. The first is the phonon scattering length of the electrons, which is proportional to $1/T$, and the other is the amount of conduction bands available, which is proportional to T.[24] For our samples, the latter appears to be dominant, resulting in a reduction of CNT via resistance with increasing substrate temperature.

With the resistance and TCR known, the 3ω-measurements can be performed. For accurate measurements, it is necessary to select the appropriate excitation frequency and current range for the applied sinusoid current. The frequency has to be selected in a way that the CNT are not excited at a resonant frequency of the circuit, and where the reactance is zero. As is shown in Fig. 4, the samples show no resonant peaks, due to the excellent shielding of the probe station. The resistance is the most stable in the range of 100 Hz to 10 kHz. The current should be low enough so it does not induce an excessive amount of self-heating in the bundle, which will result in an error due to radiative losses,[21] while still inducing a measurable third harmonic.

In order for Eq. (1) to be valid, the frequency has to be selected in such a way that the measurement is performed in the low frequency limit: $\lambda \gg L$, in which λ is the thermal wavelength as specified as $\lambda = \sqrt{\alpha/2\omega}$, where α is the thermal diffusivity.[21] The mass density of the CNT is estimated to be 261 kg/m^3 by calculating the mass of a single CNT and the bundle density.[25] The specific heat of MWCNT bundles has been shown to be close to that of graphite (0.7 J/gK).[26] If we assume κ to be in the range of 1−100 W/mK, then α ranges from 5.5×10^{-6} m^2/s to 5.5×10^{-4} m^2/s. For the length of our CNT bundles (2.6 μm), this would put us in the low frequency limit for frequencies of 1 kHz or lower.

Figure 5 displays the measured third harmonic voltage from CNT vias with a width of either 2 μm or 4 μm. The data were fitted to a power-law using least-squares fitting, as indicated by the solid lines. As can be seen, the fitted power-law indices are close to the theoretical value of $n = 3$. For the 4 μm sample, a clear deviation from the predicted behaviour can be observed for higher currents, which is likely caused

Downloaded 04 Jul 2013 to 131.180.130.178. This article is copyrighted as indicated in the abstract. Reuse of AIP content is subject to the terms at: http://apl.aip.org/about/rights_and_permissions

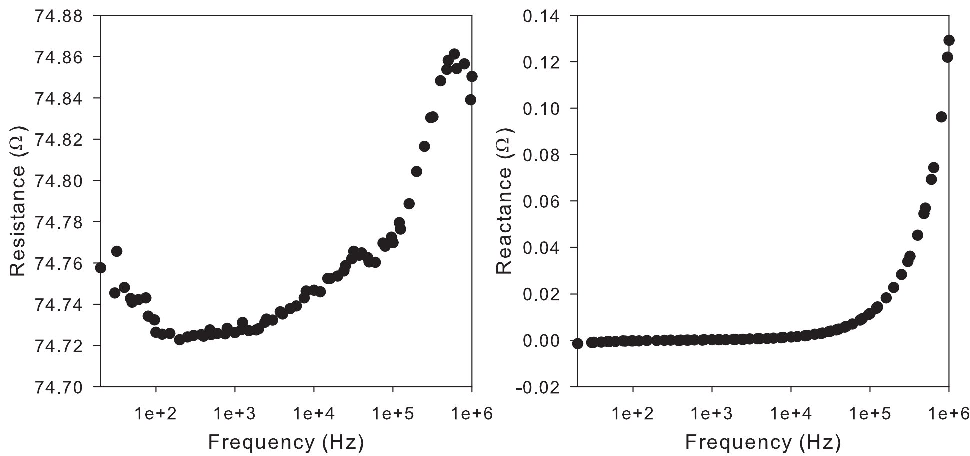

FIG. 4. Impedance spectra of a typical 2 μm wide via obtained using a LCR-meter.

by self-heating of the sample. We expect that this is also the cause for the larger deviation from $n = 3$ of the 2 μm sample. However, at lower currents, the $V_{3\omega}$ cannot be accurately measured.

Using the TCR and $V_{3\omega}$ measurement data, together with Eq. (1), the thermal conductivities of the CNT inside the bundle can be obtained. The bundle length was set at 2.6 μm. As the CNT bundle is sparse, the actual cross-sectional area is not equal to that of the hole etched in the oxide. The following equation was used to determine the cross-sectional diameter of the bundle ($A_{CNT,bundle}$):

$$A_{CNT,bundle} = \frac{\pi d^2}{4} D w^2 \tag{2}$$

in which d is the average CNT diameter (14 nm), D is the density (10^{11} tubes/cm^2), and w is the width of the opening. For the measured bundles, this results in a κ of 3.5 and 1.7 W/mK for, respectively, the 2 and 4 μm wide bundles.

These values are much lower than values reported before obtained from CNT fabricated at higher temperatures, which are typically tens to many hundreds W/mK.[14–18] There are several explanations for this. First of all, the measured values include the thermal contact resistance between the metal contact and the CNT bundle. While we found previously that the electrical contact resistance is low,[20] this does not necessarily mean that the thermal contact resistance is low as well. More importantly, the growth temperature used to fabricate these CNT is much lower than those used to fabricate CNT measured before in literature. From Raman spectroscopy and electrical measurements, we estimated the electron mean free path (mfp) to be in the order of 5 nm,[20] much lower than reported values as high as 25 μm.[27] The reported thermal conductivity here is close to those reported before for carbon nanofibres, which indeed were found to have a short phonon mfp of just a few nm,[10] even though our sample consists of CNT as confirmed by TEM analyses elsewhere.[20]

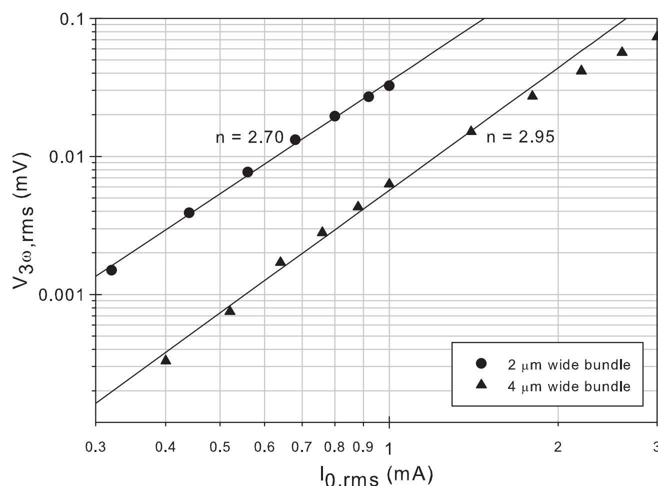

FIG. 5. Measured third harmonic as function of the applied current.

Finally, we discuss the validity of our measurement. First of all, no phase change was measured by the lock-in amplifier, confirming the measurement was performed in the low frequency limit.[21] Whereas in regular 3ω measurements the CNT (bundle) is orientated horizontally over a gap in vacuum[8,11,13,18] these bundles are vertically oriented between two metal heat sinks and isolated from thermal conduction by a (vacuum) gap. Although the exact orientation of the bundle, of course, does not influence the measurements, the heat sinking properties of the contacts may be different. Equation (1) only holds in case the contacts are thermal sinks at temperature (close to) T_0. While we can expect this to hold for the bottom contact, as it is in direct contact with the Si bulk, this is not necessarily the case for the top contact.

Finite element simulations were performed by COMSOL MULTIPHYSICS 4.3 to verify the potential increase of temperature of the top contact. A cross-section model was constructed for this, and the thermal conductivity of the CNT bundle was modelled as a solid, with a thermal conductivity determined from the measurements assuming a solid material. This results in a thermal conductivity of about 0.5 W/mK. For all other materials, the bulk conductivities were assumed.

Figure 6 displays the simulation results for a 4 μm wide via with a maximum current density equal to an I_0 of 1 mA. As can be seen from Fig. 6(a), the heat is localized inside the bundle. In Fig. 6(b), the temperature against time at three different locations (centre of the bundle, top contact 100 nm from bundle, and bottom contact 100 nm from bundle) are displayed. As can be seen, the two contacts only display a minor increase of temperature (<0.1 K), which are moreover close to each other. Finally, the self-heating of the CNT bundle is small. If the current is increased to 2 mA instead, the maximum temperature in the centre increases to 307.5 K and goes up rapidly for even higher currents. This confirms that

Downloaded 04 Jul 2013 to 131.180.130.178. This article is copyrighted as indicated in the abstract. Reuse of AIP content is subject to the terms at: http://apl.aip.org/about/rights_and_permissions

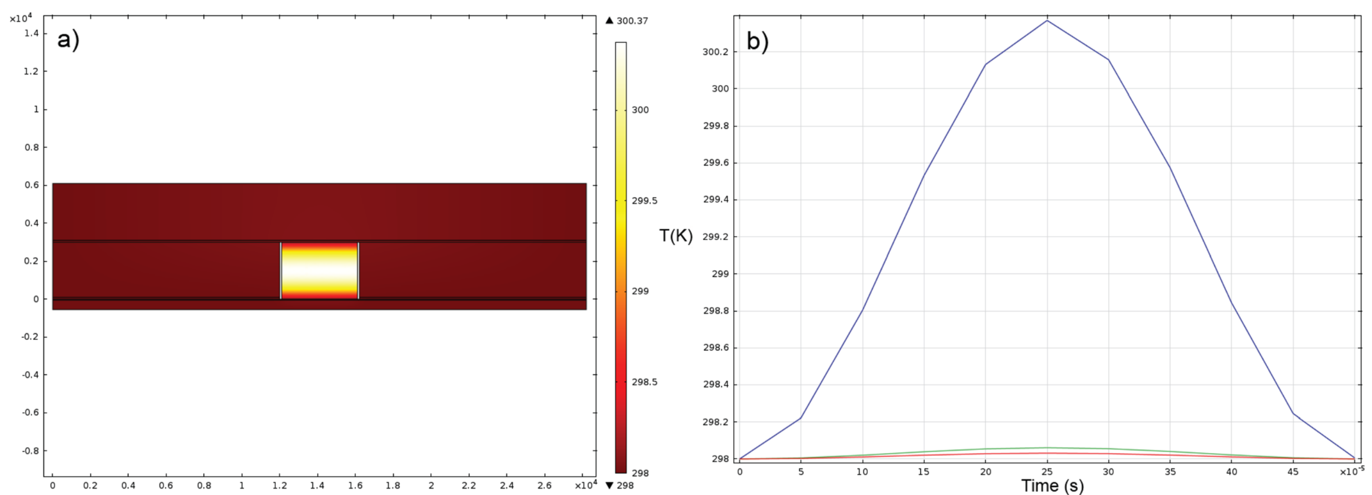

FIG. 6. Finite element simulation of via cross-section: (a) temperature distribution at peak of sinusoid current, (b) temperature at different locations in cross-section: centre of bundle (blue line), bottom electrode (red line), and top electrode (green line).

self-heating is most likely the cause of the deviation from $n = 3$ as observed in Fig. 5 for the 4 μm bundle at higher currents.

In summary, vertically aligned carbon nanotubes grown at low temperature (500 °C) were thermally characterised. For this, a vertical 3ω-method was employed. Both the measurements and simulations point out the validity of this method. The obtained thermal conductivity of individual multi-walled CNT (1.7–3.5 W/mK) was found to be much lower than values reported before in literature for high quality tubes. The low quality of the sample, due to the low growth temperature, is the likely cause of this. This implies that CNT quality will be crucial in order to allow CNT to outperform current materials. Effort should be put in optimizing growth conditions in order to obtain sufficient quality even at low growth temperature.

Part of the work has been performed in the project JEMSiP_3D, which is funded by the Public Authorities in France, Germany, Hungary, The Netherlands, Norway, and Sweden, as well as by the ENIAC Joint Undertaking. The authors would like to thank Ann N. Chiaramonti from the National Institute of Standards and Technology (NIST, Boulder, CO, USA) for making the dual-beam FIB/SEM cross-section sample and image.

[1]J. Robertson, Mater. Today **10**, 36 (2007).
[2]N. Srivastava, H. Li, F. Kreupl, and K. Banerjee, IEEE Trans. Nanotechnol. **8**, 542 (2009).
[3]K. Kordás, G. Tóth, P. Moilanen, M. Kumpumäki, J. Vähäkangas, A. Uusimäki, R. Vajtaia, and P. M. Ajayan, Appl. Phys. Lett. **90**, 123105 (2007).
[4]H. Huang, C. H. Liu, Y. Wu, and S. Fan, Adv. Mater. **17**, 1652 (2005).
[5]T. Tong, Y. Zhao, L. Delzeit, A. Kashani, M. Meyyappan, and A. Majumdar, IEEE Trans. Compon. Packag. Technol. **30**, 92 (2007).
[6]K. Zhang, Y. Chai, M. M. F. Yuen, D. G. W. Xiao, and P. C. H. Chan, Nanotechnology **19**, 215706 (2008).
[7]X. J. Hu, A. A. Padilla, J. Xu, T. S. Fisher, and K. E. Goodson, J. Heat Transfer **128**, 1109 (2006).
[8]W. Yi, L. Lu, Z. Dian-lin, Z. W. Pan, and S. S. Xie, Phys. Rev. B **59**, R9015 (1999).
[9]P. Kim, L. Shi, A. Majumdar, and P. L. McEuen, Phys. Rev. Lett. **87**, 215502 (2001).
[10]C. Yu, S. Saha, J. Zhou, L. Shi, A. M. Cassell, B. A. Cruden, Q. Ngo, and J. Li, J. Heat Transfer **128**, 234 (2006).
[11]T. Y. Choi, D. Poulikakos, J. Tharian, and U. Sennhauser, Nano Lett. **6**, 1589 (2006).
[12]E. Pop, D. Mann, Q. Wang, K. Goodson, and H. Dai, Nano Lett. **6**, 96 (2006).
[13]Z. L. Wang, D. W. Tang, X. B. Li, X. H. Zheng, W. G. Zhang, L. X. Zheng, Y. T. Zhu, A. Z. Jin, H. F. Yang, and C. Z. Gu, Appl. Phys. Lett. **91**, 123119 (2007).
[14]J. Hone, M. Whitney, and A. Zettl, Synth. Mater. **103**, 2498 (1999).
[15]D. J. Yang, Q. Zhang, G. Chen, S. F. Yoon, J. Ahn, S. G. Wang, Q. Zhou, Q. Wang, and J. Q. Li, Phys. Rev. B **66**, 165440 (2002).
[16]M. Horibe, M. Nihei, D. Kondo, A. Kawabata, and Y. Awano, Jpn. J. Appl. Phys., Part 1 **43**, 7337 (2004).
[17]H. Xie, A. Cai, and X. Wang, Phys. Lett. A **369**, 120 (2007).
[18]A. E. Aliev, M. H. Lima, E. M. Silverman, and R. H. Baughman, Nanotechnology **21**, 035709 (2010).
[19]S. Vollebregt, R. Ishihara, J. Derakhshandeh, J. van der Cingel, H. Schellevis, and C. I. M. Beenakker, in *11th IEEE Conference on Nanotechnology* (2011), pp. 985–990.
[20]S. Vollebregt, A. N. Chiaramonti, R. Ishihara, H. Schellevis, and C. I. M. Beenakker, in *12th IEEE Conference on Nanotechnology* (2012), pp. 424–428.
[21]L. Lu, W. Yi, and D. L. Zhang, Rev. Sci. Instrum. **72**, 2996 (2001).
[22]T. Y. Choi, M. H. Maneshian, B. Kang, W. S. Chang, C. S. Han, and D. Poulikakos, Nanotechnology **20**, 315706 (2009).
[23]S. Vollebregt, R. Ishihara, F. D. Tichelaar, J. van der Cingel, and K. Beenakker, in *IEEE International Interconnect Technology Conference* (2012), pp. 1–3.
[24]A. Naeemi and J. D. Meindl, IEEE Electron Device Lett. **28**, 135 (2007).
[25]C. Laurent, E. Flahaut, and A. Peigney, Carbon **48**, 2994 (2010).
[26]C. Masarapu, L. L. Henry, and B. Wei, Nanotechnology **16**, 1490 (2005).
[27]Y. Li, S. Peng, D. Mann, J. Cao, R. Tu, K. J. Cho, and H. Dai, J. Phys. Chem. B **109**, 6968 (2005).

Downloaded 04 Jul 2013 to 131.180.130.178. This article is copyrighted as indicated in the abstract. Reuse of AIP content is subject to the terms at: http://apl.aip.org/about/rights_and_permissions